Cellular Signalling xxx (2013) xxx–xxx

Contents lists available at ScienceDirect

Cellular Signalling

journal homepage: www.elsevier.com/locate/cellsig

Bilirubin mediated oxidative stress involves antioxidant response activation *via* Nrf2 pathway

Mohammed Qaisiya [a,*], Carlos Coda Zabetta [a], Cristina Bellarosa [a], Claudio Tiribelli [a,b]

[a] Fondazione Italiana Fegato ONLUS, Italian Liver Foundation ONLUS, Bldg Q AREA Science Park — Basovizza Campus, 34149 Trieste, Italy
[b] Department of Medical Sciences, University of Trieste, 34100 Trieste, Italy

ARTICLE INFO

Article history:
Received 24 October 2013
Received in revised form 21 November 2013
Accepted 26 November 2013
Available online xxxx

Keywords:
Bilirubin neurotoxicity
Oxidative stress
Nrf2 pathway
Heme oxygenase 1
Antioxidant Response Element
Stress response protein kinases

ABSTRACT

Unconjugated bilirubin (UCB) is responsible for neonatal jaundice and high level of free bilirubin (Bf) can lead to kernicterus. Previous studies suggest that oxidative stress is a critical component of UCB-induced neurotoxicity. The Nrf2 pathway is a powerful sensor for cellular redox state and is activated directly by oxidative stress and/or indirectly by stress response protein kinases. Activated Nrf2 translocates to nucleus, binds to Antioxidant Response Element (ARE), and enhances the up-regulation of cytoprotective genes that mediate cell survival. The aim of the present study was to investigate the role of Nrf2 pathway in cell response to bilirubin mediated oxidative stress in the neuroblastoma SH-SY5Y cell line. Cells exposed to a toxic concentration of UCB (140 nM Bf) showed an increased intracellular ROS levels and enhanced nuclear accumulation of Nrf2 protein. UCB stimulated transcriptional induction of ARE-GFP reporter gene and induced mRNA expression of multiple antioxidant response genes as: xCT, Gly1, γGCL-m, γGCL-c, HO-1, NQO1, FTH, ME1, and ATF3. Nrf2 siRNA decreased UCB induced mRNA expression of HO1 (75%), NQO1 (54%), and FTH (40%). The Nrf2-related HO-1 induction was reduced to 60% in cells pre-treated with antioxidant (NAC) or specific signaling pathway inhibitors for PKC, P38α and MEK1/2 (80, 40 and 25%, respectively). In conclusion, we demonstrated that SH-SY5Y cells undergo an adaptive response against UCB-mediated oxidative stress by activation of multiple antioxidant response, in part through Nrf2 pathway.

1. Introduction

Bilirubin is an end product of heme catabolism possessing both cytoprotective and cytotoxic properties [1]. In mammalians bilirubin plays a major role as antioxidant at physiological concentrations [2–4]. This pigment circulates in blood bound to albumin (unconjugated bilirubin, UCB) with only a minimal free fraction known as free bilirubin (Bf) which determines the pathophysiological properties of bilirubin [5–8]. When the plasma concentration is markedly elevated, the Bf can diffuse passively across any cell membrane [9]. The most vulnerable site to UCB toxicity is the central nervous system in which the pigment produces a wide array of neurological deficits collectively known as bilirubin encephalopathy or kernicterus [7,10–12]. The molecular mechanisms of Bf induced cell injury are incompletely elucidated and although Bf diffuses into all brain regions and cells [13], it remains unknown why only certain types of cells, *e.g.* Purkinje cells [14,15] are more susceptible to UCB toxicity than other cells such as astrocytes [16].

Oxidative stress (OS) has been implicated in the progression of many neurological diseases, and a growing body of evidence suggests that OS is a hallmark of UCB induced neurotoxicity. Increased intracellular reactive oxygen species (ROS) was detected in mouse hepatoma Hepa1c1c7 cells after incubation with UCB [17,18]. HeLa and mouse embryonic cell culture exposed to UCB above its aqueous saturation (>70 nM) showed the induction of OS, promoting the intracellular accumulation of ROS which led to the activation of redox sensor proteins APE/Ref1 [19]. SH-SY5Y cells exposed to UCB induced OS and activated redox sensor protein DJ-1. Furthermore, the pre-treatment of SH-SY5Y cells with the antioxidant N-acetylcystein (NAC) resulted in a significant reduction in UCB-induced mortality [20]. Studies using primary cultures of astrocytes and neurons confirmed the role of OS in cytotoxicity mediated by UCB [16,21–24]. Higher ROS production was observed in neurons as compared to astrocytes while UCB toxicity was reduced by exogenous antioxidants [23,24].

The NF-E2-related factor 2 (Nrf2) is a master cellular sensor for OS and represents the primary response to changes in cellular redox state

Abbreviations: Bf, free bilirubin; UCB, unconjugated bilirubin; OS, oxidative stress; ROS, reactive oxygen species; NAC, N-acetylcystein; Nrf2, NF-E2 related factor 2; ARE, Antioxidant Response Element; GSH, glutathione; xCT, cystine/glutamate exchanger system; Gly1, glycine up-take transporter; γ-GCL-c, γ-glutamylcysteine synthetase, catalytic subunit; γ-GCL-m, γ-glutamylcysteine synthetase, modulatory subunit; HO-1, heme oxygenase 1; FTH, ferritin heavy chain; NQO1, NADPH quinone oxidoreductase 1; ME1, cytosolic malic enzyme 1; ATF3, activating transcription factor 3; *t*BHQ, tertiary-butylhydroquinone; PKC, protein kinase C; MAPK, mitogen-activated protein kinase; PI3K, phosphatidylinositide 3-kinases; JNK, c-Jun NH2-terminal kinases; eIF2α, eukaryotic translation initiation factor 2α; PERK, protein kinase-like endoplasmic reticulum kinase.

* Corresponding author at: Italian Liver Foundation, Bldg Q, AREA Science Park — Basovizza Campus, Ss 14, km 163.5, 34149 Trieste, Italy. Tel.: +39 040 375 7917.
E-mail addresses: m.qaisiya@csf.units.it (M. Qaisiya), carlos.zabetta@csf.units.it (C.C. Zabetta), cristina.bellarosa@csf.units.it (C. Bellarosa), ctliver@csf.units.it (C. Tiribelli).

0898-6568/$ – see front matter © 2013 Published by Elsevier Inc.
http://dx.doi.org/10.1016/j.cellsig.2013.11.029

[25–28]. Under basal state, Nrf2 is tethered within the cytosol by the inhibitory partner cysteine rich protein Keap1 and degraded by the ubiquitin-proteasome system [29]. Nrf2 pathway is activated directly by OS and/or indirectly by stress-response protein kinases such as protein kinase C (PKC), mitogen activated protein kinase (MAPK) cascade, phosphatidylinositide 3-kinases (PI3K) [26,30,31], and protein kinase-like endoplasmic reticulum kinase (PERK) [32]. Activated Nrf2 accumulates in the nucleus and binds to the Antioxidant Response Element (ARE) [25], a *cis*-acting enhancer present in the promoter region of a large and distinct set of target genes, which aims to restore redox homeostasis [33–36].

One main feature of Nrf2 activation is the up-regulation of its target genes that involved in: (1) Glutathione (GSH) homeostasis such as: cysteine uptake transporter (xCT) [37], glycine uptake transporter (Gly1) [38], and the rate limiting enzyme of GSH synthesis; γ-glutamylcysteine ligase catalytic and modulatory subunits (γ-GCL-c and γ-GCL-m, respectively) [39,40]. (2) Antioxidant and detoxification such as: heme oxygenase 1 (HO-1) [41,42], ferritin heavy chain (FTH) [43], and NADPH-Quinone oxidoreductase 1 (NQO1) [44,45]. (3) NADPH homeostasis such as malic enzyme (ME1) [38,46]. (4) Stress response such as activating transcription factor 3 (ATF3) [47].

In the present study, we have tested the effects of UCB on Nrf2 pathway in SH-SY5Y cells and the changes in gene expression, with focus on antioxidant/stress response genes. We have also investigated the genes induced by UCB at Nrf2 dependent manner and the signaling pathways involved in Nrf2/HO-1 pathway activation.

2. Materials and methods

2.1. Cells culture and UCB treatment

SH-SY5Y cells were maintained in EMEM/F12 1:1 supplemented with 15% fetal bovin serum (FBS), 1% penicillin streptomycin solution (100 U/mL penicillin, 100 mg/mL streptomycin), 2 mM L-glutamine and 1% non-essential amino acids (Sigma Aldrich, USA). HepG2 cells were maintained in DMEM supplemented with 10% FBS and 1% penicillin streptomycin solution and 1% glutamine. The concentration of UCB required to reach the desired Bf concentration (140 nM) was calculated according to protocol by Roca et al. [48] obtained by adding a stock solution of UCB in DMSO in the medium and verified spectrophotometrically at 468 nm. Control experiments were performed by exposing the cells to the same final concentration of DMSO in the medium. Cells treated with *t*BHQ (Sigma Aldrich, USA), a potent activator of Nrf2 pathway, were used as a positive control [36]. *t*BHQ was dissolved in DMSO: PBS (1:10) and added to a final concentration in the medium.

2.2. Determination of intracellular ROS level

The intracellular ROS accumulation after UCB treatment was determined using the 2′7′-dichlorofluorescein diacetate (DCFH-DA) compound. 60.000 cells/cm^2 were seeded in 6 multi-well plates and grown to 70% confluence. Cells were pre-treated for 15 min with 10 μM DCFH-DA diluted in serum free medium with 25 mM Hepes, and exposed to a 140 nM Bf for 1 h. Cells treated with 0.6% DMSO or 0.2 mM H_2O_2 were used as negative and positive controls, respectively. At the end of the treatment, cells were washed with PBS, detached by trypsinization and re-suspended in PBS for FACS analysis. The intensity of fluorescence was measured with a BD FACS Callibur (Becton Dickinson, Franklin Lakes, NJ, USA) and analyzed with CellQuest Pro software.

2.3. Nuclear protein extractions, quantification, and Western blot analysis

SH-SY5Y cells at 80% confluence were treated with 140 nM Bf (equivalent to 30 μM UCB) in a time dependent manner for 1 h, 3 h, 6 h, and 24 h, with 50 μM *t*BHQ for 3 h, and with 0.6% DMSO for 3 h. Nuclear extracts were obtained using a minor modification of Dignam's method [49] as we described previously [19]. Protein content was determined by the Bicinchoninic Acid Protein Assay (BCA) using bovine serum albumin as standard [50]. Purity of cytoplasmic-nuclear protein extracts were analyzed by SDS-PAGE using αP84 nuclear matrix protein marker antibodies (Abcam Inc., Cambridge, MA, USA) (data not shown). Rabbit polyclonal anti-Nrf2 antibody (Santa Cruz Biotechnology Inc., USA) was used to detect Nrf2 by SDS–PAGE in 10% acrylamide gel. The actin expression was assessed using rabbit polyclonal anti-actin antibodies (Sigma Aldrich, USA). Anti-rabbit HRP-conjugated (Dako laboratories, Denmark) was used as secondary antibody. The peroxidase reaction was obtained using ECL-Plus Western Blotting detection system solutions (Amersham–PharmaciaBiotech, UK). For HepG2 experiment, cells at 80% confluence were treated with 100 μM UCB for 1 h, 3 h, 6 h, and 24 h with 100 μM *t*BHQ for 3 h, and with 1.8% DMSO for 3 h. Nuclear proteins extraction and Western blot were performed as described above. The optical density of protein bands was analyzed using the NIH Image software (Scion Corporation Frederick, MD, USA), normalized to α-actin protein density, and represented as protein relative expression.

2.4. RNA extraction and reverse transcriptase-real time PCR (qRT-PCR)

SH-SY5Y cells at 80% confluence were exposed to the following experimental conditions: 0.6% DMSO or 140 nM Bf for 4 h, 8 h, 16 h, and 24 h. Total RNA was isolated using EuroGOLD RNAPure™ according to the manufacture's suggestions (Euro Clone, Italy). The total RNA concentration and purity were quantified by spectrophotometry (DU®730, Beckman Coulter, Milan, Italy). For each samples, the A_{260}/A_{280} ratio between 1.6 and 2.0 was considered as good RNA quality. cDNA was obtained from 1 μg of purified RNA using the High Capacity cDNA Reverse Transcription Kits (Applied Biosystems, USA) according to the manufacture's suggestions. The reaction was run in a thermalcycler (Gene Amp PCR System 2400, Perkin-Elmer, Boston, MA, USA) following the reaction protocol proposed by the manufacturer. qPCR was performed according to the iQ SYBR Green Supermix (Bio-Rad Laboratories, Hercules, CA, USA) protocol. PCR amplification was carried out in 25 μL reaction volume containing 25 ng of cDNA, 1× iQ SYBR Green Supermix (100 mM KCl; 40 mM Tris-HCl; pH: 8.4; 0.4 mM each dNTP; 40 U/mL iTaq DNA polymerase; 6 mM $MgCl_2$; SYBR Green I; 20 mM fluorescein; and stabilizers) (Bio-Rad) and 250 nM of gene specific forward and reverse primers. qPCR reaction was run in IQ5 real time PCR system (Bio-Rad). Primer sequences designed using Beacon Designer 4.02 software (PREMIER Biosoft International, Palo Alto, CA, USA) are listed in (Table 1). Cycling parameters were determined and the results were

Table 1
List of forward and reverse primers designed for qRT-PCR analysis.

Target gene	Accession number	Forward primers 5′-3′	Reverse primers 5′-3′
γGCL-c	NM_001498.3	AATGTCCGAGTTCAATAC	AATCTGGGAAATGAAGTTAT
γGCL-m	NM_002061.2	ATCAAACTCTTCATCATCAAC	GATTAACTCCATCTTCAATAGG
xCT	NM_014331.3	GGTGGTGTGTTTGCTGTC	GCTGGTAGAGGAGTGTGC
Gly 1	NM_201649.2	CTTCTCCTTGGTGGTCAT	CATCTGGATGTCCTGGAA
HO-1	NM_002133.2	ATGCCCCAGGATTTGTCA	CCCTTCTGAAAGTTCCTCAT
FTH	NM_002032.2	TTACCTGTCCATGTCTTAC	TCATCAGTTTCTCAGCAT
NQO-1	NM_000903.2	CCTCTATGCCATGAACTT	TATAAGCCAGAACAGACTC
ME1	NM_002395.4	CGGCAGAGAAGAGTAAGA	ACTTGTTCAGGAGACGAA
ATF3	NM_001674.3	AAAAGAGGCGACGAGAAA	CAGCATTCACACTTTCCAG
GAPDH[a]	NM_002046.4	TCAGCCGCATCTTCTTTTG	GCAACAATATCCACTTTACCAG
HPRT[a]	NM_000194…	ACATCTGGAGTCCTATTGACATCG	CCGCCCAAAGGGAACTGATAG

[a] Housekeeping genes used for normalizing the expression of target genes.

Please cite this article as: M. Qaisiya, et al., Cellular Signalling (2013), http://dx.doi.org/10.1016/j.cellsig.2013.11.029

analyzed by using the comparative Ct method as the means of relative quantification, normalized to two references genes (GAPDH and HPRT) and expressed as $2^{-\Delta\Delta CT}$. Melting curve analysis was performed to assess product specificity.

2.5. Cell transfection and ARE-GFP reporter gene assay

The Cignal™ Antioxidant Response Reporter Kit (SABiosciences; Frederick, MD, USA) utilizes Monster Green Fluorescence protein (GFP) under the control of ARE enhancers (ARE-GFP construct) was used to monitor the signal activation of ARE through Nrf2 according to handbook instructions. A constitutively expressing GFP construct (CMV-GFP) was used to set transfection conditions and efficiency. A reporter gene under the control of basal promoter element (TATA-GFP) was used as negative control. The GFP fluorescence intensity was analyzed by fluorescence microscope (Nikon eclipse TS100, Nikon instruments Europe B.V., Netherlands) (excitation filter 470 ± 20 nm and emission filter 515 nm). GFP signal was quantified using flow cytometry FACS Calibur of an argon laser (488 nm excitation and filter 530 ± 15 emission) and analyzed with CellQuest Pro software. Percentage of GFP positive cells was calculated by dot blot show the side scattered detector-highet (SSC-H) blotted with GFP fluorescence detector-highet (FL1). Percentage of fluorescence in negative controls was considered as basal auto fluorescence value. Constructs were transiently transfected into SH-SY5Y cells using Lipofectamine™ Reagent (Invitrogen; Merelbeke, Belgium) according to the manufacturer's recommendation. The best conditions were obtained when cells are transfected at 80% confluent with 0.8 μg DNA: 3 μL lipofectamin in Opti-MEM® I reduced serum medium (Invitrogene, Italy) for 6 h. Medium was replaced with fresh complete medium for additional 24 h. Transfection efficiency obtained was 50–60% calculated by FACS analysis after 48 h post-transfection (data not shown). For treatment experiments, cells were transfected with proper construct (ARE-GFP or TATA-GFP) for 24 h then incubated with assay medium containing 1% FBS for additional 8 h. 32 h post-transfection, cells were treated with 50 μM *t*BHQ or 140 nM Bf for 24 h and stimulation was allowed to proceed for additional 16 h before analysis.

2.6. Nrf2 siRNA

The experimentally validated Nrf2 siRNA (SI03246950, Qiagen, USA) was used to knockdown Nrf2 expression. siRNA against non target mRNA was used as negative control (1027310, Qiagene). siRNA was transfected using siLentFect™ Lipid reagent (Bio-Rad) according to the manufacturer's recommendation. SH-SY5Y cells at 60% confluence were transfected with 50 nM of siRNA in the presence of 3 μL siLentFect reagent for 48 h and siRNA efficiency was analyzed by qRT-PCR. For treatment experiments, after 48 h siRNA transfection the cells were treated with 0.6% DMSO or 140 nM Bf for additional 24 h and genes expression were analyzed by qRT-PCR. For viability assay, cells transfected with siRNA were pre-treated or not-treated with 0.1 mM BSO for 2 h, followed by incubation with 0.6% DMSO, or 0.2 mM H_2O_2, or 140 nM Bf for additional 24 h (BSO was maintained during incubation time), and cells viability were determined by 3(4,5-dimethylthiazolyl-2)-2,5 diphenyl tetrazolium (MTT) assay [51].

2.7. NAC treatment and applying of signaling pathways inhibitors

SH-SY5Y cells at 80% of confluence were pre-treated for 1 h with exogenous antioxidant NAC (0.5 mM) or with specific signaling pathway inhibitors: PI3K inhibitor LY-294002 (10 μM), MEK1/2 (or MAPK kinase 2) inhibitor PD 98059 (20 μM), c-Jun NH2-terminal kinases (JNK) inhibitor SP 600125 (10 μM), p38α (or MAPK14) inhibitor SB 203580 (10 μM) and PKC inhibitor GF 109203X (10 μM). Concentration of inhibitors was used as described by others [52]. Beside the GF 109203X which was purchased from Cyaman Chemicals (Italy), all other inhibitors were obtained from Selleckchem (Italy). After 1 h, cells were exposed to 0.6% DMSO or 40 nM Bf (negative control) or 0.2 mM H_2O_2 (positive control) or 140 nM Bf for additional 16 h in the presence or absence of NAC or specific inhibitors (NAC and specific inhibitors were maintained during incubation time). The expression of HO-1 was analyzed by qRT-PCR.

2.8. Statistics

Data were obtained from at least three independent experiments and are expressed as mean ± SD. Statistical analysis was performed using student's *t*-test. $P < 0.05$ was considered as significant.

3. Results

3.1. UCB increases ROS, up-regulates Nrf2 mRNA and enhances nuclear accumulation of Nrf2 protein

Previous studies from our group established the neuroblastoma SH-SY5Y cells as a suitable cellular model to study the molecular mechanisms of UCB induced neurotoxicity [53]. In the present work we observed an increased level of intracellular ROS in cells treated with 140 nM Bf (1.9 folds) as compared to those treated with 0.6% DMSO for 60 min; cells treated with 0.2 mM H_2O_2 for 60 min (1.5 folds) were used as positive control (Fig. 1A). As ROS is a direct activator of Nrf2 pathway, we investigated whether UCB-mediated ROS generation also activates Nrf2 pathway. SH-SY5Y cells treated with 140 nM Bf (equivalent to 30 μM UCB) showed an up-regulation of Nrf2 mRNA expression after 8 h maintained until 16 h (1.7 fold and 2.2 folds, respectively). This up-regulation disappeared after 24 h indicating the transient induction of the Nrf2 gene (Fig. 1B). When Nrf2 proteins translocation was measured by Western blot analysis, a nuclear accumulation of Nrf2 protein (100 KDa) was found after Bf treatment with a peak increment between 3 h (4.7 folds) and 6 h (6.6 folds); the return to basal occurred at 24 h (0.7 fold). 50 μM of *t*BHQ, an Nrf2 activator used as positive control, also increased the nuclear accumulation (4.3 folds) of Nrf2 proteins after 3 h of treatment while cells incubated with 0.6% DMSO for 3 h show no bands for the protein (Fig. 1C and D). When similar experiments were performed on HepG2 cells, the exposure to 100 μM UCB showed a time dependent increase of nuclear Nrf2 proteins starting after 1 h with a maximum between 3 h (2 folds) to 6 h (3.9 folds) and the return to basal level at 24 h. 100 μM of *t*BHQ increased Nrf2 nuclear proteins after 3 h of treatment (2.3 folds) while no nuclear proteins were detected in cell incubated with 1.8% DMSO (Fig. 1E and F).

3.2. UCB induces ARE-GFP reporter gene expression in SH-SY5Y cells

To confirm that the accumulated nuclear Nrf2 protein is transcriptionally active toward ARE, a reporter gene composed of GFP under the control of ARE *cis*-elements repeats was used. SH-SY5Y cells transfected with ARE-GFP constructs were treated with 0.6% DMSO (negative control), 50 μM *t*BHQ (positive control), or 140 nM Bf (Fig. 2A). Green fluorescence protein (GFP) was detected by immunofluorescence microscopy (IF) in cells treated with *t*BHQ and Bf while no signal was detected in DMSO-treated cells (Fig. 2A. upper panel). The percentage of GFP positive cells quantified by FACS analysis 35% in *t*BHQ and 46% in Bf treated cells, compared to 5% (basal fluorescence) in DMSO treated cells (Fig. 2A. lower panel). Cells transfected with TATA-GFP constructs treated with 50 μM *t*BHQ (negative control) showed 7% of basal fluorescence while cells transfected with CMV-GFP constructs showed 80% of GFP positive, were used as positive controls for GFP signal (Fig. 2B).

Please cite this article as: M. Qaisiya, et al., Cellular Signalling (2013), http://dx.doi.org/10.1016/j.cellsig.2013.11.029

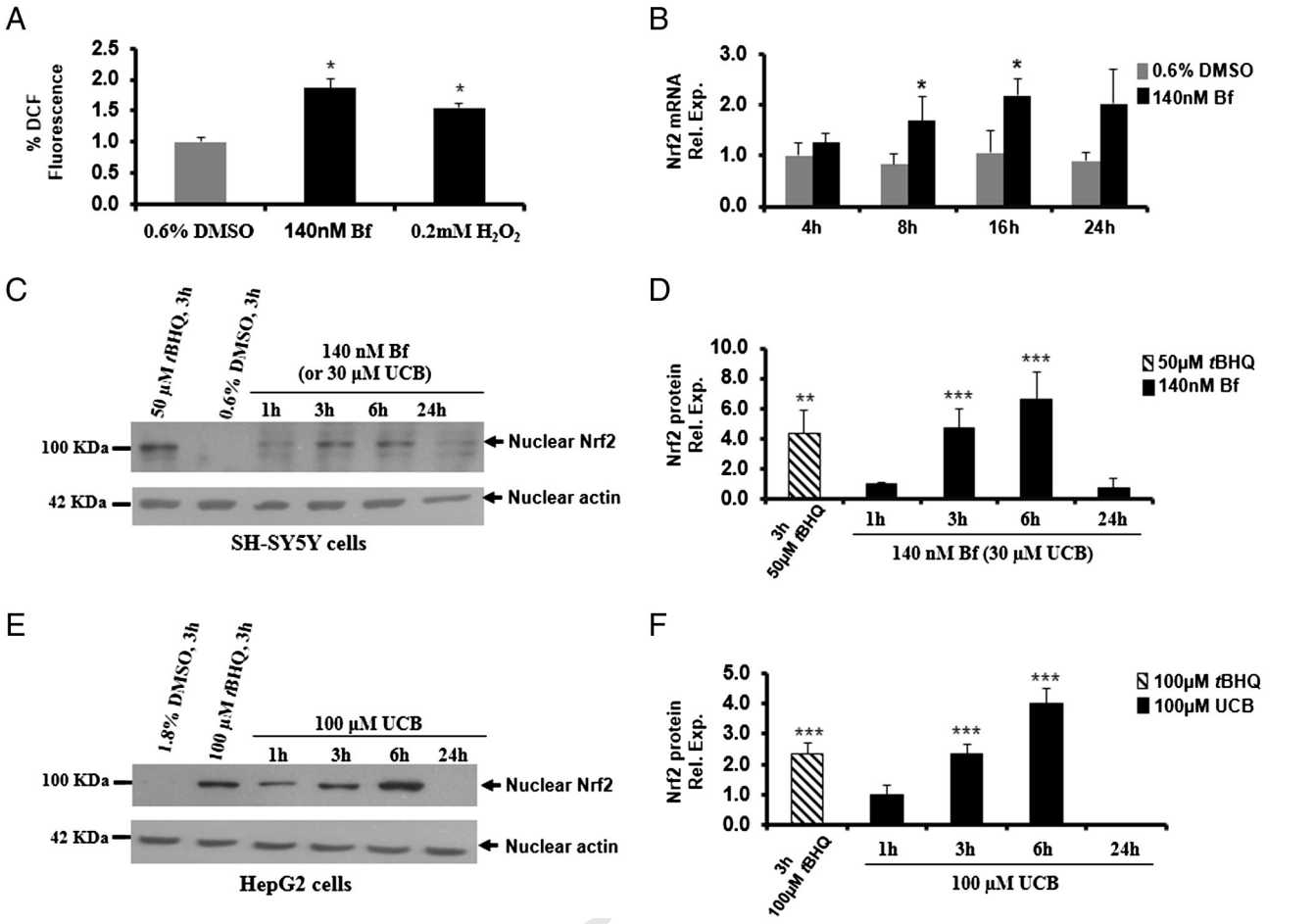

Fig. 1. UCB increases oxidative stress and enhances nuclear accumulation of Nrf2 protein. (A) Intracellular ROS level in SH-SY5Y cells treated with 0.6% DMSO (control), 140 nM Bf, and 0.2 mM H_2O_2 (positive control) for 1 h. (B) Relative expression of Nrf2 mRNA in SH-SY5Y cells treated with 140 nM Bf or vehicle (0.6% DMSO) at indicated times. (C) Representative Western Blot of Nrf2 (100KDa) and α-actin (42KDa) proteins in nuclear extracts from SH-SY5Y cells treated with 0.6% DMSO for 3 h (negative control), 50 μM *t*BHQ for 3 h (positive control), and 140 nM Bf (30 μM UCB) for 1 h, 3 h, 6 h, and 24 h. (D) Protein quantification: the optical density of Nrf2 protein was normalized to the density of α-actin protein and reported as relative expression to cells incubated with 140 nM Bf for 1 h. Quantification is the mean of three independent experiments (**$P < 0.01$; ***$P < 0.001$). (E) Representative Western Blot of Nrf2 (100KDa) and α-actin (42KDa) proteins in HepG2 cells treated with 1.8% DMSO for 3 h (negative control), 100 μM *t*BHQ for 3 h (positive control), and 100 μM UCB for 1 h, 3 h, 6 h, and 24 h. (F) Protein quantification: the density of Nrf2 protein was normalized to the density of α-actin protein, and represented as the relative expression to cells incubated with 100 μM UCB for 1 h. Quantification is the mean of three independent experiments.

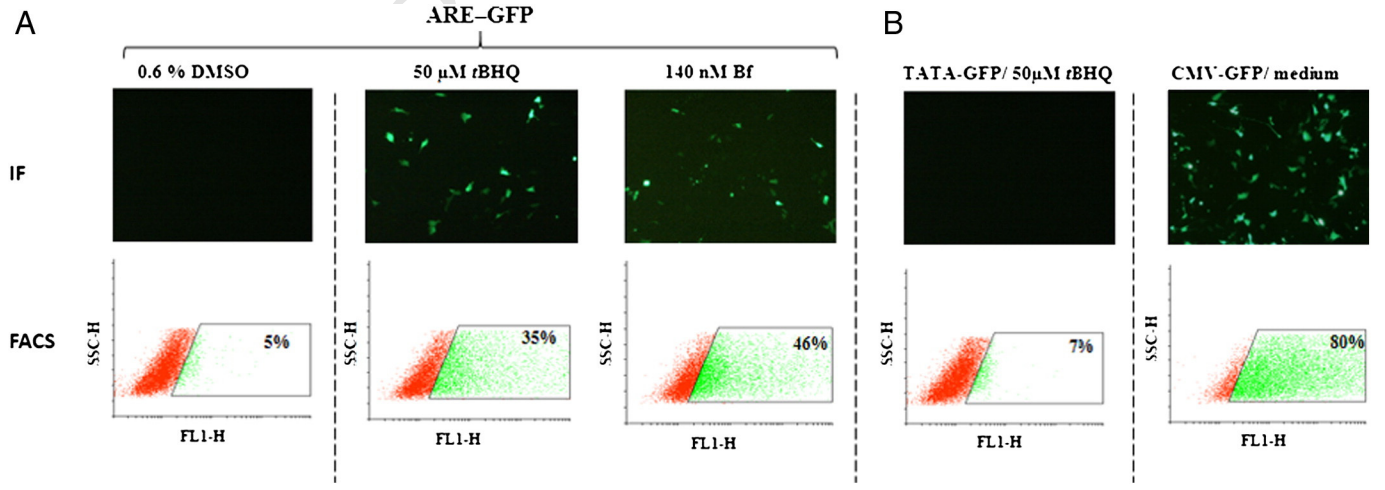

Fig. 2. UCB activates Nrf2 pathway and induces expression of ARE-GFP reporter gene in SH-SY5Y cells. (A) Cells transfected with ARE-GFP reporter were treated with 0.6% DMSO (control), or 50 μM *t*BHQ (positive control), or 140 nM Bf for 24 h (left panel). After 40 h of stimulation, GFP signal was visualized by immunofluorescence microscopy (IF, upper panel) and quantified using FACS analysis (Dot blot histogram show the side scattered detector-highet (SSC-H) blotted with GFP fluorescence detector-highet (FL1)) (lower panel). Microscope magnification: objective 20×. (B) Cells transfected with negative control (TATA-GFP) show a low percentage of basal fluorescence, while cells transfected with (CMV-GFP) were used as positive control for GFP signal.

Please cite this article as: M. Qaisiya, et al., Cellular Signalling (2013), http://dx.doi.org/10.1016/j.cellsig.2013.11.029

3.3. mRNA expression of Nrf2 target genes in SH-SY5Y cells treated with UCB

In order to correlate the Nrf2 pathway activation with mRNA expression of its target genes, qRT-PCR analysis was performed. Data were collected in a time dependent manner (4, 8, 16, and 24 h) to investigate both early (4 to 8 h) and late (16 to 24 h) response genes. Compared to DMSO control, cells treated with 140 nM Bf showed a significant up-regulation of mRNA expression of different genes as ATF3 (8 folds) at 4 h; xCT (10 folds) and Gly1 (13 folds) at 8 h; γGCL-c (2 folds), HO-1 (30 folds), and NQO-1 (2 folds) at 16 h; γGCL-m (3 folds), FTH (3 folds), and ME1 (2.5 folds) at 24 h (Table 2).

3.4. Effects of Nrf2 siRNA on genes induction and cell viability upon UCB exposure

To identify the genes up-regulated by UCB at Nrf2 dependent manner, we used specific siRNA to knockdown Nrf2 mRNA expression. 50 nM Nrf2 siRNA down-regulated Nrf2 mRNA to about 60% as compared to 50 nM control siRNA (Fig. 3A). After 48 h of transfection, cells were treated with 0.6% DMSO or 140 nM Bf for additional 24 h for gene analysis. The functionality of Nrf2 siRNA was confirmed by analyzing the basal expression of HO-1 and NQO1, which were reduced by Nrf2 siRNA to about 40% in DMSO-treated cells (Fig. 3B and C). Upon UCB exposure, the induction of HO-1 was decreased by 75% (Fig. 3B) and that of NQO1 by 54% (Fig. 3C) in the Nrf2 siRNA transfected cell as compared to control siRNA. Interestingly, even though no change on the basal expression of FTH was observed, the induction of FTH was reduced by 40% (Fig. 3D). No change was detected in xCT, Gly1, γGCL-c, γGCL-m, ME1, and ATF3 expressions at basal or UCB-induced state (data not shown).

To test whether Nrf2 siRNA affects cell viability upon UCB exposure, cells transfected with control siRNA or Nrf2 siRNA were treated with DMSO 0.6%, 0.2 mM H_2O_2 (positive control) or 140 nM Bf for 24 h; cell viability was assessed by MTT assay. In control siRNA transfected cells 0.2 mM H_2O_2 and 140 nM Bf reduced cell viability to 71% and 68%, respectively. Nrf2 siRNA further reduced cell viability to 51% upon H_2O_2 exposure while no change was detected in Bf treated cells. (Fig. 4, left panel).

We hypothesize that the cells were able to maintain redox state through the induction of Nrf2-independent genes mainly those involved in GSH homeostasis. siRNA transfected cells were pre-treated with 0.1 mM BSO (a specific inhibitor for γGCL) for 2 h followed by exposure to 0.6% DMSO, 0.2 mM H_2O_2, or 140 nM Bf for additional 24 h. In Nrf2 siRNA transfected cells, BSO treatment further reduced cell viability to 36% and 43% after exposure to 0.2 mM H_2O_2 and 140 nM Bf as compared to 66% and 70% in control siRNA (Fig. 4, right panel). Cells transfected with control siRNA or Nrf2 siRNA, incubated with BSO and treated with 0.6% DMSO were used as controls and showed about 95% and 90% of cell viability, respectively, (not significant compared to cells not treated with BSO (100%) (Fig. 4).

3.5. HO-1 induction by UCB involves oxidative stress

Among the different genes analyzed, HO-1 was highly induced by 140 nM Bf treatment and its expression was mainly dependent on Nrf2. In order to clarify the contribution of OS in the activation of Nrf2/HO-1 axis, SH-SY5Y cells were pre-treated with exogenous antioxidant (0.5 mM NAC) before Bf exposure. HO-1 mRNA expression was induced 3 folds in SH-SY5Y cells treated with 0.2 mM H_2O_2 (positive control), but only 1.5 folds in the presence of NAC. Similarly, HO-1 mRNA expression was induced 25 folds by 140 nM Bf treatment and 10 folds in the presence of NAC. Cells treated with 0.6% DMSO or 0.5 mM NAC or with a non-toxic concentration of Bf (40 nM) were used as controls (Fig. 5).

3.6. HO-1 induction involves activation of different stress response protein kinases

To investigate the upstream signaling pathway(s) involved in Nrf2/HO-1 induction by Bf, the same approach was proceeded using different inhibitors. Results demonstrated that the HO-1 mRNA expression was 45 folds induced in cells treated with 140 nM Bf respect to controls, while the induction was reduced to 9 folds, 27 folds, and 34 folds in the presence of PKC, P38α, and MEK1/2 inhibitors, respectively (Fig. 6). The expression was not changed using inhibitors for JNK and PI3K pathways.

4. Discussion

Cell response to oxidative stress (OS) mainly depends by cell type, the nature of toxic compound, and the outcome of signaling pathways. OS induces multiple cellular signal transduction (sensors) that determine cell fate. Cells unable to restore homeostasis proceed to apoptosis while cell survival depends on the ability of cells to restore homeostasis and resist the stress. This is why mammalian cells have developed redox sensitive proteins that aim to restore cellular redox state and provide cell survival [54,55]. Among all, Nrf2 pathway represents the primary response to OS and has attracted attention as a promising target to counteract neurological diseases due to its potent ability to up-regulate cytoprotective enzymes [35,56–58]. The molecular mechanisms of UCB induced neurotoxicity are still incompletely elucidated. However, changes of cellular redox state by UCB appear to play an important role in mediating cell damage.

Table 2
mRNA expression of Nrf2 target genes candidate.

mRNA[a]	Early response				Late response			
Genes	4 h		8 h		16 h		24 h	
	0.6% DMSO	140 nM Bf	0.6% DMSO	140 nM Bf	0.6% DMSO	140 nM Bf	0.6% DMSO	140 nM Bf
γGCL-c	1	1 ± 0.1	1.2 ± 0.2	1.1 ± 0.1	1.2 ± 0.2	**2 ± 0.2****	1.5 ± 0.1	1.4 ± 0.5
γGCL-m	1	1 ± 0.1	1 ± 0.4	1.2 ± 0.3	0.9 ± 0.2	**3 ± 0.3*****	1 ± 0.3	**3 ± 0.8***
xCT	1	3 ± 2	1.1 ± 0.7	**10 ± 3***	0.8 ± 0.5	**20 ± 2.2*****	0.8 ± 0.2	**8 ± 0.8****
Gly1	1	1.6 ± 0.3	2 ± 1.3	**13 ± 3***	1 ± 0.1	**13 ± 4.8*****	1.2 ± 0.3	**14 ± 2.5****
HO-1	1	1.6 ± 0.3	1.7 ± 0.7	3.9 ± 1.8	1 ± 0.6	**30 ± 7.5****	1 ± 0.5	**32 ± 8.2****
FTH	1	1 ± 0.1	0.8 ± 0.3	0.8 ± 0.2	1 ± 0.2	1.9 ± 0.7	1 ± 0.3	**3 ± 0.6***
NQO-1	1	1 ± 0.4	1 ± 0.3	1 ± 0.4	1 ± 0.3	**2 ± 0.6***	1 ± 0.5	**5 ± 0.6*****
ME1	1	1 ± 0.2	0.9 ± 0.3	1.3 ± 0.1	0.9 ± 0.2	1.7 ± 0.4	1.2 ± 0.1	**2.5 ± 0.1*****
ATF3	1	**8 ± 2.5****	1.8 ± 1.4	**39 ± 11****	1 ± 0.3	**42 ± 8****	1 ± 0.3	**31 ± 5*****

[a] Values represented relative mRNA expressions of Nrf2 target genes candidate (γGCL-c, γGCL-m, xCT, Gly1, HO1, FTH, NQO1, ME1, and ATF3) in SH-SY5Y cells treated with 0.6% DMSO or 140 nM Bf for 4 h, 8 h, 16 h and 24 h. Statistically significant (*$P < 0.05$, **$P < 0.01$, ***$P < 0.001$) up-regulations were underlined and highlighted in bold. The mRNA expression was normalized to housekeeping genes and expressed as relative to cells treated with 0.6% DMSO at the same time.

Please cite this article as: M. Qaisiya, et al., Cellular Signalling (2013), http://dx.doi.org/10.1016/j.cellsig.2013.11.029

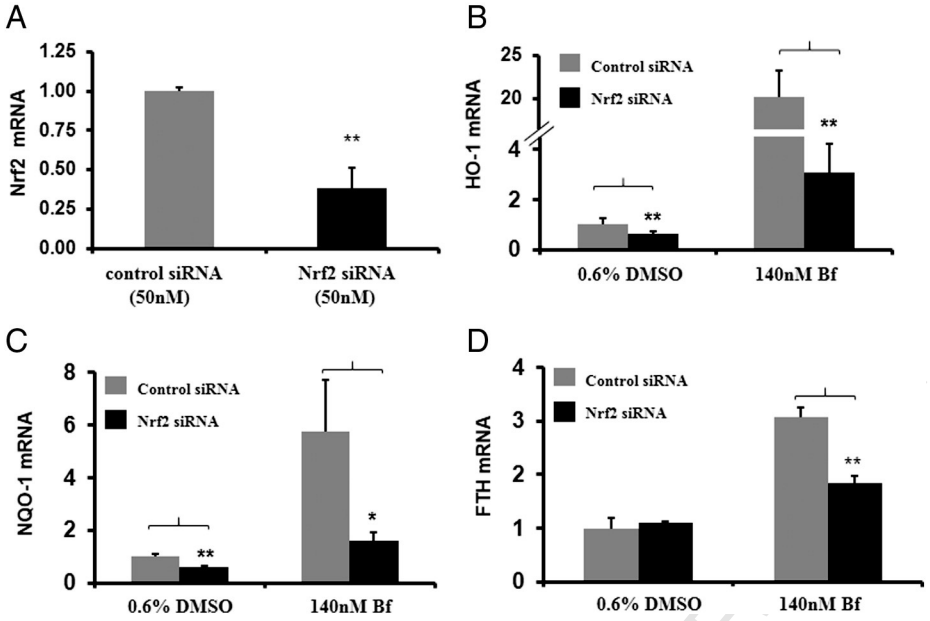

Fig. 3. Nrf2 siRNA decreases the induction of HO-1, NQO1, and FTH by UCB. (A) Effects of 50 nM of negative control siRNA or Nrf2 siRNA on Nrf2 mRNA expression after 48 h of transfection. (B) Expression of HO-1, NQO1, and FTH in SH-SY5Y cells transfected with control siRNA or Nrf2 siRNA and then treated with 0.6% DMSO or 140 nM Bf for additional 24 h.

4.1. Nrf2 activation in response to oxidative stress mediated by UCB

We have previously demonstrated the involvement of OS in mediating cell death by UCB in SH-SY5Y cells [20] but shown that the cell was able to overcome UCB toxicity [53]. In the present study, we hypothesized and explored if SH-SY5Y cells may undergo an adaptive response against OS through Nrf2 pathway activation. An increased intracellular level of ROS was detected in cells after 1 h of UCB treatment which was associated with a rapid and early nuclear accumulation of Nrf2 and followed by an increase of Nrf2 mRNA expression. To confirm whether the UCB-induced nuclear accumulation of Nrf2 is not restricted to SH-SY5Y cells, we repeat the same experiment in HepG2 cells. Hepatocytes represent a well-known model to study the molecular mechanisms of cell resistance to UCB toxicity, and can tolerate a UCB concentration three times higher than that causing neurotoxicty [59]. HepG2 cells treated with UCB increased the nuclear accumulation of Nrf2 proteins and showed an up-regulation of HO-1 and NQO1 (data not shown), suggesting the activation of Nrf2 pathway. A recent study demonstrated that UCB causes nuclear translocation of Nrf2 protein in primary culture of mouse hepatocytes [60]. The activation of Nrf2 pathway in hepatic derived cells is expected since many members of cytochrome P450 (CYPs) were suggested to play a major role in bilirubin oxidation [61,62]. Furthermore, CYP catalytic activity is the major system for ROS generation [63] that may directly activate Nrf2 pathway [64].

4.2. UCB mediates transcriptional activation of ARE and up-regulation of its target genes candidate

To confirm Nrf2 pathway activation in SH-SY5Y cells we used a reporter gene assay of GFP under the control of ARE enhancer. GFP signal was increased in response to UCB exposure indicating that the accumulated nuclear Nrf2 protein was transcriptionally active toward ARE element. In line with this observation, we detected an up-regulation of several Nrf2 candidate genes upon UCB treatment. When we analyzed these genes in terms of time of response, they may be divided into two main categories: early (4 h–8 h) and late response (16 h–24 h). As far as early genes, UCB mediated a sequential transcription starting

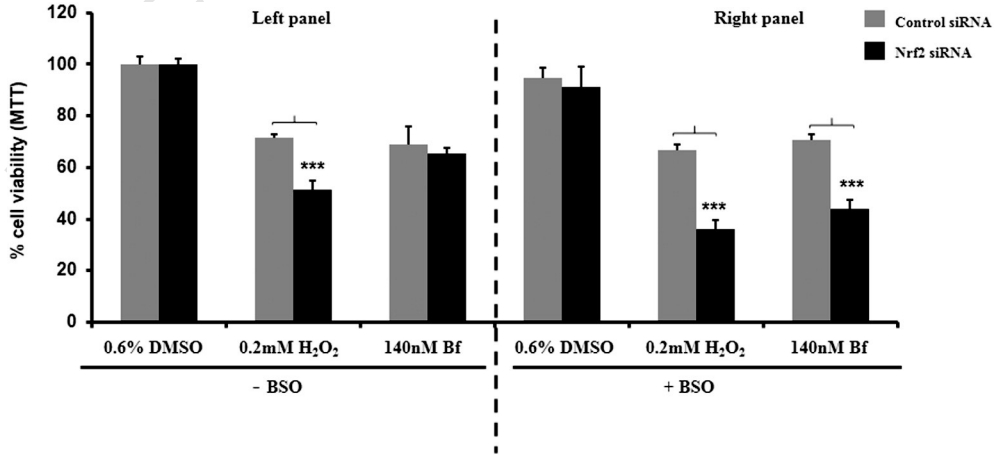

Fig. 4. Nrf2 siRNA combined with BSO treatment sensitize SH-SY5Y cells to UCB toxicity. Cell viability (MTT) in SH-SY5Y cells transfected with control siRNA or Nrf2 siRNA with (right panle) and without (left panel) pre-treatment of 0.1 mM BSO for 2 h (+BSO and −BSO, respectively) before 0.6% DMSO, or 0.2 mM H_2O_2, or 140 nM Bf exposure for additional of 24 h (BSO was maintained during 24 h).

Please cite this article as: M. Qaisiya, et al., Cellular Signalling (2013), http://dx.doi.org/10.1016/j.cellsig.2013.11.029

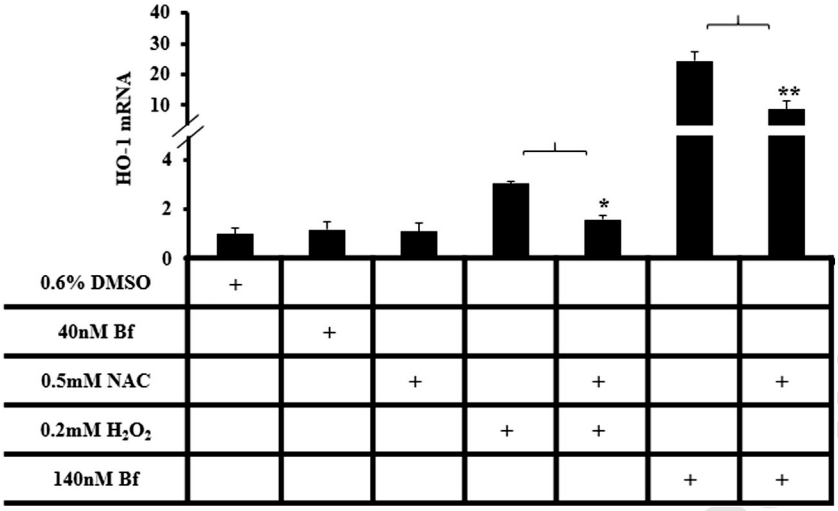

Fig. 5. Antioxidant NAC reduces the induction of HO-1 by UCB. HO-1 mRNA expression after 16 h in SH-SY5Y cells treated with 0.6% DMSO (control); 40 nM Bf (negative control); 0.5 mM NAC (control); 0.2 mM H_2O_2 (positive control) or 140 nM Bf in the absence or presence of 0.5 mM NAC.

with the ATF3 up-regulation at 4 h and followed by the induction of amino acid transporters at 8 h (xCT and Gly1). On the contrary, for late genes, we observed up-regulation of the enzymes involved in GSH synthesis (γGCL) and antioxidant/detoxification (HO-1, NQO1, FTH, and ME1). These results indicated that the cells exposed to UCB aim to restore cellular redox state through the induction of several antioxidant response genes and that this response is time-related.

4.3. Nrf2 siRNA reduces the induction of only of HO-1, NQO1, and FTH and by itself is not sufficient to increase cell sensitivity to UCB toxicity

Knockdown of Nrf2 mRNA led to reduced HO-1 and NOQ-1 induction by UCB indicating that Nrf2 is involved in the transcription of these genes. On the contrary, Nrf2 silencing did not affect the UCB-induced expression of ATF3, xCT, Gly1, γGCL and ME1 (data not shown), suggesting that other signaling are involved in the transcriptional regulation of these genes. It is possible that the reduction of FTH induction by UCB was due to the down-regulation of HO-1 rather than to the direct effect of Nrf2 siRNA, since FTH expression is usually coordinated with HO-1 expression [65].

We also tested whether Nrf2 silencing affects the cell sensitivity to oxidative damage induced by UCB. Nrf2 siRNA sensitized cells to H_2O_2 but not to UCB toxic effects, suggesting that other pathway(s) may compensate the loss of Nrf2. One possible candidate is the GSH. Previous studies demonstrated that resistance to GSH depletion involves Nrf2/HO-1 activation [66], while increased levels of GSH reduced Nrf2/HO-1 activation [67]. These data suggest a cross talk between Nrf2/HO-1 and GSH cycle. We hypothesize that SH-SY5Y cells transfected with Nrf2 siRNA were still able to maintain redox state through GSH-homeostasis enzymes upon UCB exposure. Supporting this hypothesis our previous results demonstrating that SH-SY5Y cells exposed to UCB show an increased level of intracellular GSH [68]. In addition, the present data show that the induction of genes involved in GSH homeostasis occurred at Nrf2-independent manner. When cells transfected with siRNA were incubated with BSO (a specific inhibitor for GSH synthesis), cells became more sensitive to UCB toxicity, pointing

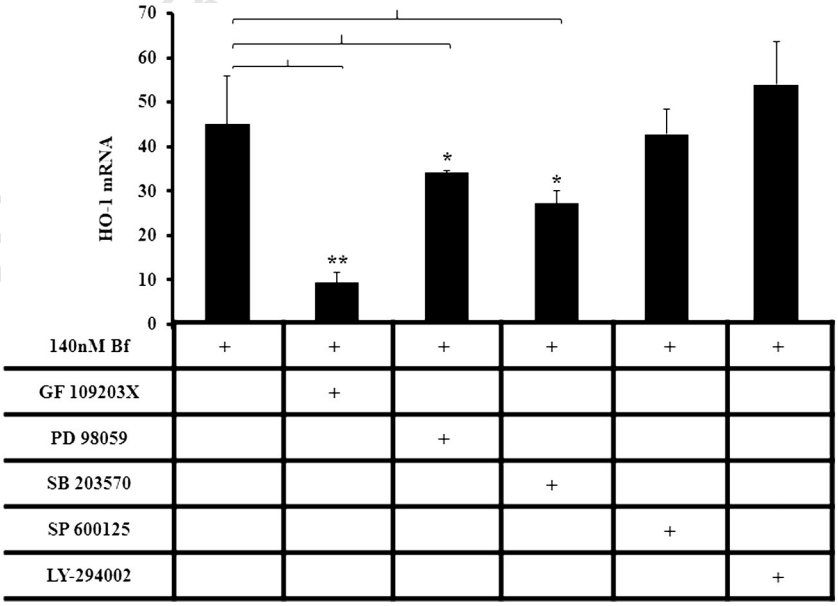

Fig. 6. Effects of different signaling kinases inhibitors on HO-1 induction by UCB. HO-1 mRNA expression after 16 h in SH-SY5Y cells treated with 140 nM Bf in the absence or presence of specific signaling pathway inhibitors: PKC (GF 109203X), MEK1/2 (PD 98059), p38α (SB 203570), JNK (SP 600125), and PI3K (LY-294002). Relative expression was normalized to cells incubated only with vehicles composed of 0.6% DMSO or specific chemical inhibitors alone.

Please cite this article as: M. Qaisiya, et al., Cellular Signalling (2013), http://dx.doi.org/10.1016/j.cellsig.2013.11.029

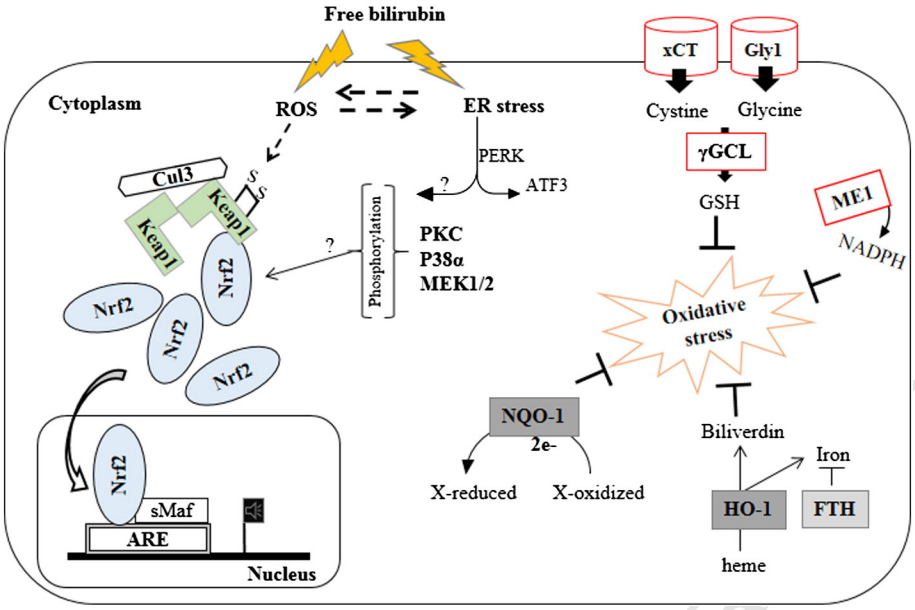

Fig. 7. Proposed model of UCB mediating OS and activation of antioxidant response in SH-SY5Y cells. UCB mediated oxidative stress, enhanced the nuclear accumulation of Nrf2 and induction of ARE. UCB induced expression of several antioxidant-stress response genes, among all, HO-1 and NQO1 were up-regulated by UCB at Nrf2 dependent manner (highlighted with gray box color) while others (highlighted with red box color) are involved in another transcriptional machinery, most probably, through ER stress transcription factors. Nrf2-related HO-1 induction by UCB involved oxidative stress and stress response protein kinases (mainly PKC).

to the involvement of both Nrf2 and GSH in cellular redox homeostasis upon UCB exposure.

4.4. Oxidative stress and PKC are the major signaling involved in the activation of Nrf2/HO-1 axis

Our results showed that HO-1 was highly induced by UCB and its induction was mainly dependent on Nrf2. This allowed us to identify the up-stream molecular mechanisms involved in Nrf2/HO-1 axis activation. HO-1 is a sensitive and fairly ubiquitous marker for OS [69–71]. When OS was reduced by treating cells with NAC (a glutathione precursor), a down-regulation of HO-1 expression was observed indicating the involvement of OS in Nrf2/HO-1 activation. Furthermore, HO-1 is widely accepted as a *bona fide* to detect the activated signaling pathways upon OS [72,73]. However, cells type and nature of chemical inducer determine the specific activation of certain protein kinases [54,74]. Limited information is available regarding the signaling pathways activated by UCB and their contribution in mediating neuronal cell survival or toxicity. The maximal reduction of HO-1 induction (80%) in SH-SY5Y cells treated with PKC inhibitor suggest that this signaling is the main pathway involved in HO-1 induction by UCB. The reduction of HO-1 induction by P38α (40%), and MEK-ERK1/2 (25%) inhibitors further indicated the activation of these signaling pathways by UCB and their partial contribution in HO-1 induction, while PI3K and JNK signaling appeared not to be involved in HO-1 induction by UCB.

4.5. ATF3 up-regulation represents the earliest response to UCB toxicity

From the present data, it is evident that ATF3 up-regulation at 4 h represents the earliest response to UCB exposure an occurred at Nrf2 independent manner. This gene is induced by several stimuli [75] and is a putative marker of ER stress [76]. ATF3 together with other ER stress biomarkers (ATF4 and CHOP) are induced in coordination with mechanisms requiring the phosphorylation of eIF2α by activated PERK [76,77]. We previously demonstrated that activation of ER stress components is the main response mediated by UCB in SH-SY5Y cells but were unable to detect an early response (4 h) by microarray approach [53]. By the more sensitive qRT-PCR analysis we detected an up-regulation of ER stress biomarkers upon UCB exposure at 4 h (ATF4, 2 fold, and CHOP, 6 folds) followed at 8 h by XBP1 (11 folds), ATF6 (2 folds), and GRP78 (4 folds (data not shown). In addition, our data suggest that ER stress (via PERK activation) represents the earliest response to UCB toxicity in SH-SY5Y cellular model. Since PERK activation leads to Nrf2 pathway activation under ER stress [32], we can hypothesize that ER stress works synergistically to activate Nrf2 pathway by UCB. A logic scenario may include calcium release under ER stress, generation of ROS [78], and activation of PKC/Nrf2/HO-1 pathway [79].

We have previously reported that UCB treatment causes a reduced progression of the cell through S-phase associated to increased cell death by apoptosis [20]. We hypothesize that these two events are linked to ER stress and to the oxidative damage that mediates CHOP expression (linked to apoptosis) and translation inhibition (phosphorylation of eIF2α, loss of cyclin D1 protein, and cell cycle arrest).

In summary, we demonstrated that SH-SY5Y cells undergo an adaptive response - against UCB induced OS - through activation of multiple antioxidant response, in part *via* Nrf2 pathway (Fig. 7). Our data indicate the activation of endogenous antioxidants as a fundamental system to reduce UCB toxicity involved OS and ER stress in SH-SY5Y cells.

Statement of financial support

This work was supported by the Regione Friuli Venezia Giulia-Italy (Fondo Regionale FVG lR26/2005), Telethon grant (GGP10051), and AREA Science Park (PhD fellowship to Mohammed Qaisiya).

Acknowledgments

The authors thank Prof. Richard Wennberg and Dr. Yaqoub Ashhab for critical reading of the manuscript.

References

[1] J. Kapitulnik, Mol. Pharmacol. 66 (2004) 773–779.
[2] R. Stocker, Y. Yamamoto, A.F. McDonagh, A.N. Glazer, B.N. Ames, Science 235 (1987) 1043–1046.
[3] M.L. Tomaro, A.M. Batlle, Int. J. Biochem. Cell Biol. 34 (2002) 216–220.
[4] D.E. Baranano, M. Rao, C.D. Ferris, S.H. Snyder, Proc. Natl. Acad. Sci. U. S. A. 99 (2002) 16093–16098.

Q2
[5] J.D. Ostrow, P. Mukerjee, C. Tiribelli, J. Lipid Res. 35 (1994) 1715–1737.
[6] C.E. Ahlfors, J. Perinatol. 21 (Suppl. 1) (2001) S40–S42.
[7] J.D. Ostrow, L. Pascolo, S.M. Shapiro, C. Tiribelli, Eur. J. Clin. Invest. 33 (2003) 988–997.
[8] J.D. Ostrow, P. Mukerjee, C. Tiribelli, J. Lipid Res. 35 (1994) 1715–1737.
[9] S.D. Zucker, W. Goessling, A.G. Hoppin, J. Biol. Chem. 274 (1999) 10852–10862.
[10] G.R. Gourley, Adv. Pediatr. 44 (1997) 173–229.
[11] S.M. Shapiro, V.K. Bhutani, L. Johnson, Clin. Perinatol. 33 (2006) 387–410.
[12] J.F. Watchko, Neuromolecular Med. 8 (2006) 513–529.
[13] S. Gazzin, J. Zelenka, L. Zdrahalova, R. Konickova, C.C. Zabetta, P.J. Giraudi, et al., Pediatr. Res. 71 (2012) 653–660.
[14] H. Keino, H. Sato, R. Semba, S. Aono, E. Aoki, S. Kashiwamata, Pediatr. Neurosci. 12 (1985) 145–150.
[15] J.W. Conlee, S.M. Shapiro, Acta Neuropathol. 93 (1997) 450–460.
[16] M.A. Brito, A.I. Rosa, A.S. Falcao, A. Fernandes, R.F. Silva, D.A. Butterfield, et al., Neurobiol. Dis. 29 (2008) 30–40.
[17] J.M. Seubert, A.J. Darmon, A.O. El-Kadi, S.J. D'Souza, J.R. Bend, Mol. Pharmacol. 62 (2002) 257–264.
[18] G.H. Oakes, J.R. Bend, J. Biochem. Mol. Toxicol. 19 (2005) 244–255.
[19] L. Cesaratto, S.D. Calligaris, C. Vascotto, M. Deganuto, C. Bellarosa, F. Quadrifoglio, et al., J. Mol. Med. 85 (2007) 1099–1112.
[20] M. Deganuto, L. Cesaratto, C. Bellarosa, R. Calligaris, S. Vilotti, G. Renzone, et al., Proteomics 10 (2010) 1645–1657.
[21] M.A. Brito, D. Brites, D.A. Butterfield, Brain Res. 1026 (2004) 33–43.
[22] M.A. Brito, S. Lima, A. Fernandes, A.S. Falcao, R.F. Silva, D.A. Butterfield, et al., Neurotoxicology 29 (2008) 259–269.
[23] A.R. Vaz, S.L. Silva, A. Barateiro, A.S. Falcao, A. Fernandes, M.A. Brito, et al., Mol. Cell. Neurosci. 48 (2011) 82–93.
[24] R.F. Silva, C.M. Rodrigues, D. Brites, J. Hepatol. 34 (2001) 402–408.
[25] K. Itoh, T. Chiba, S. Takahashi, T. Ishii, K. Igarashi, Y. Katoh, et al., Biochem. Biophys. Res. Commun. 236 (1997) 313–322.
[26] K. Itoh, K.I. Tong, M. Yamamoto, Free Radic. Biol. Med. 36 (2004) 1208–1213.
[27] T.W. Kensler, N. Wakabayashi, S. Biswal, Annu. Rev. Pharmacol. Toxicol. 47 (2007) 89–116.
[28] S.K. Niture, J.W. Kaspar, J. Shen, A.K. Jaiswal, Toxicol. Appl. Pharmacol. 244 (2010) 37–42.
[29] K. Itoh, N. Wakabayashi, Y. Katoh, T. Ishii, K. Igarashi, J.D. Engel, et al., Genes Dev. 13 (1999) 76–86.
[30] M.K. Kwak, N. Wakabayashi, T.W. Kensler, Mutat. Res. 555 (2004) 133–148.
[31] D.D. Zhang, Drug Metab. Rev. 38 (2006) 769–789.
[32] S.B. Cullinan, J.A. Diehl, J. Biol. Chem. 279 (2004) 20108–20117.
[33] L. Baird, A.T. Dinkova-Kostova, Arch. Toxicol. 85 (2011) 241–272.
[34] K.A. Jung, M.K. Kwak, Molecules 15 (2010) 7266–7291.
[35] M.J. Calkins, D.A. Johnson, J.A. Townsend, M.R. Vargas, J.A. Dowell, T.P. Williamson, et al., Antioxid. Redox Signal. 11 (2009) 497–508.
[36] J. Li, D. Johnson, M. Calkins, L. Wright, C. Svendsen, J. Johnson, Toxicol. Sci. 83 (2005) 313–328.
[37] H. Sasaki, H. Sato, K. Kuriyama-Matsumura, K. Sato, K. Maebara, H. Wang, et al., J. Biol. Chem. 277 (2002) 44765–44771.
[38] J.M. Lee, M.J. Calkins, K. Chan, Y.W. Kan, J.A. Johnson, J. Biol. Chem. 278 (2003) 12029–12038.
[39] A.C. Wild, J.J. Gipp, T. Mulcahy, Biochem. J. 332 (Pt 2) (1998) 373–381.
[40] H.R. Moinova, R.T. Mulcahy, J. Biol. Chem. 273 (1998) 14683–14689.
[41] J. Alam, D. Stewart, C. Touchard, S. Boinapally, A.M. Choi, J.L. Cook, J. Biol. Chem. 274 (1999) 26071–26078.
[42] J. Sun, H. Hoshino, K. Takaku, O. Nakajima, A. Muto, H. Suzuki, et al., EMBO J. 21 (2002) 5216–5224.
[43] E.C. Pietsch, J.Y. Chan, F.M. Torti, S.V. Torti, J. Biol. Chem. 278 (2003) 2361–2369.
[44] T.H. Rushmore, M.R. Morton, C.B. Pickett, J. Biol. Chem. 266 (1991) 11632–11639.
[45] A.K. Jaiswal, Biochemistry 30 (1991) 10647–10653.
[46] K.C. Wu, J.Y. Cui, C.D. Klaassen, Toxicol. Sci. 123 (2011) 590–600.
[47] K.H. Kim, J.Y. Jeong, Y.J. Surh, K.W. Kim, Nucleic Acids Res. 38 (2010) 48–59.
[48] L. Roca, S. Calligaris, R.P. Wennberg, C.E. Ahlfors, S.G. Malik, J.D. Ostrow, et al., Pediatr. Res. 60 (2006) 724–728.
[49] J.D. Dignam, R.M. Lebovitz, R.G. Roeder, Nucleic Acids Res. 11 (1983) 1475–1489.
[50] P.K. Smith, R.I. Krohn, G.T. Hermanson, A.K. Mallia, F.H. Gartner, M.D. Provenzano, et al., Anal. Biochem. 150 (1985) 76–85.
[51] P.R. Twentyman, M. Luscombe, Br. J. Cancer 56 (1987) 279–285.
[52] K. Genc, M.Y. Egrilmez, S. Genc, Cell Biochem. Funct. 28 (2010) 197–201.
[53] R. Calligaris, C. Bellarosa, R. Foti, P. Roncaglia, P. Giraudi, H. Krmac, et al., BMC Genomics 10 (2009) 543.
[54] J.L. Martindale, N.J. Holbrook, J. Cell. Physiol. 192 (2002) 1–15.
[55] D. Trachootham, W. Lu, M.A. Ogasawara, R.D. Nilsa, P. Huang, Antioxid. Redox Signal. 10 (2008) 1343–1374.
[56] M. Zhang, C. An, Y. Gao, R.K. Leak, J. Chen, F. Zhang, Prog. Neurobiol. 100 (2013) 30–47.
[57] H.E. de Vries, M. Witte, D. Hondius, A.J. Rozemuller, B. Drukarch, J. Hoozemans, et al., Free Radic. Biol. Med. 45 (2008) 1375–1383.
[58] J.A. Johnson, D.A. Johnson, A.D. Kraft, M.J. Calkins, R.J. Jakel, M.R. Vargas, et al., Ann. N. Y. Acad. Sci. 1147 (2008) 61–69.
[59] A. Granato, G. Gores, M.T. Vilei, R. Tolando, C. Ferraresso, M. Muraca, Gut 52 (2003) 1774–1778.
[60] S.D. Kim, M. Antenos, E.J. Squires, G.M. Kirby, Toxicol. Appl. Pharmacol. 270 (2013) 129–138.
[61] A. Abu-Bakar, M.R. Moore, M.A. Lang, Biochem. Pharmacol. 70 (2005) 1527–1535.
[62] J. Kapitulnik, F.J. Gonzalez, Mol. Pharmacol. 43 (1993) 722–725.
[63] R.C. Zangar, D.R. Davydov, S. Verma, Toxicol. Appl. Pharmacol. 199 (2004) 316–331.
[64] C. Kohle, K.W. Bock, Biochem. Pharmacol. 73 (2007) 1853–1862.
[65] G.F. Vile, R.M. Tyrrell, J. Biol. Chem. 268 (1993) 14678–14681.
[66] A.L. Furfaro, J.R. Macay, B. Marengo, M. Nitti, A. Parodi, D. Fenoglio, et al., Free Radic. Biol. Med. 52 (2012) 488–496.
[67] K.J. Min, J.T. Lee, E.H. Joe, T.K. Kwon, Cell. Signal. 23 (2011) 1505–1513.
[68] P.J. Giraudi, C. Bellarosa, C.D. Coda-Zabetta, P. Peruzzo, C. Tiribelli, PLoS One 6 (2011) e29078.
[69] S.M. Keyse, R.M. Tyrrell, Proc. Natl. Acad. Sci. U. S. A. 86 (1989) 99–103.
[70] M.L. Ferrandiz, I. Devesa, Curr. Pharm. Des. 14 (2008) 473–486.
[71] W. Stefan, R.M.T. Ryter, Oxidative Stress Signal Transduct. (1997) 343–386.
[72] A. Paine, B. Eiz-Vesper, R. Blasczyk, S. Immenschuh, Biochem. Pharmacol. 80 (2010) 1895–1903.
[73] J.S. Lee, Y.J. Surh, Cancer Lett. 224 (2005) 171–184.
[74] H.O. Pae, Y.C. Lee, H.T. Chung, Recent Patents Inflamm. Allergy Drug Discov. 2 (2008) 159–165.
[75] T. Hai, C.D. Wolfgang, D.K. Marsee, A.E. Allen, U. Sivaprasad, Gene Expr. 7 (1999) 321–335.
[76] H.Y. Jiang, S.A. Wek, B.C. McGrath, D. Lu, T. Hai, H.P. Harding, et al., Mol. Cell. Biol. 24 (2004) 1365–1377.
[77] S. Oyadomari, M. Mori, Cell Death Differ. 11 (2004) 381–389.
[78] J.D. Malhotra, R.J. Kaufman, Antioxid. Redox Signal. 9 (2007) 2277–2293.
[79] S.K. Niture, A.K. Jain, A.K. Jaiswal, J. Cell Sci. 122 (2009) 4452–4464.

Please cite this article as: M. Qaisiya, et al., Cellular Signalling (2013), http://dx.doi.org/10.1016/j.cellsig.2013.11.029